

## LETTERS

## How Neanderthal molar teeth grew

Roberto Macchiarelli<sup>1</sup>, Luca Bondioli<sup>2</sup>, André Debénath<sup>3</sup>, Arnaud Mazurier<sup>1,4</sup>, Jean-François Tournepic<sup>5,6</sup>, Wendy Birch<sup>7</sup> & Christopher Dean<sup>7</sup>

Growth and development are both fundamental components of demographic structure and life history strategy. Together with information about developmental timing they ultimately contribute to a better understanding of Neanderthal extinction. Primate molar tooth development tracks the pace of life history evolution most closely<sup>1,2</sup>, and tooth histology reveals a record of birth as well as the timing of crown and root growth. High-resolution micro-computed tomography now allows us to image complex structures and uncover subtle differences in adult tooth morphology that are determined early in embryonic development<sup>3</sup>. Here we show that the timing of molar crown and root completion in Neanderthals matches those known for modern humans but that a more complex enamel–dentine junction morphology and a late peak in root extension rate sets them apart. Previous predictions about Neanderthal growth, based only on anterior tooth surfaces<sup>4,5</sup>, were necessarily speculative. These data are the first on internal molar microstructure; they firmly place key Neanderthal life history variables within those known for modern humans.

To provide information about the morphology of the Neanderthal enamel–dentine junction (EDJ) and about the timing of crown and root formation, we selected two minimally worn molars from the site

of La Chaise-de-Vouthon, Charente, France<sup>6</sup>: a lower right deciduous second molar (S14-5) from the Riss III level (OIS 6) of Abri Suard, and a lower left permanent first molar (BD-J4-C9) from the Riss-Würm level (OIS 5e) of Abri Bourgeois-Delaunay (Supplementary Information).

A record of growth exists in the enamel and dentine that allows us to reconstruct their developmental history and the timing of crown and root formation<sup>7,8</sup>. Some morphological features of the crown are the result of superficial overgrowths at the enamel surface toward the end of formation as a result of a longer secretory lifespan of ameloblasts. Others have an earlier developmental history and are mapped out at the EDJ in the embryonic tooth germ<sup>3</sup>. These are formed under the control of a signalling centre, the enamel knot, which directs differential proliferation and folding along the inner enamel epithelium<sup>9,10</sup>.

We first used high-resolution synchrotron radiation micro-computed tomography (SR- $\mu$ CT) images to reveal the EDJ within both Neanderthal molars (Fig. 1). The Neanderthal metaconid or mid-trigonid crest, a typically diagnostic feature of Neanderthal molars<sup>11</sup>, emerges as a distinct structure that is initially defined during early tooth germ development. This seems to be associated with a generally

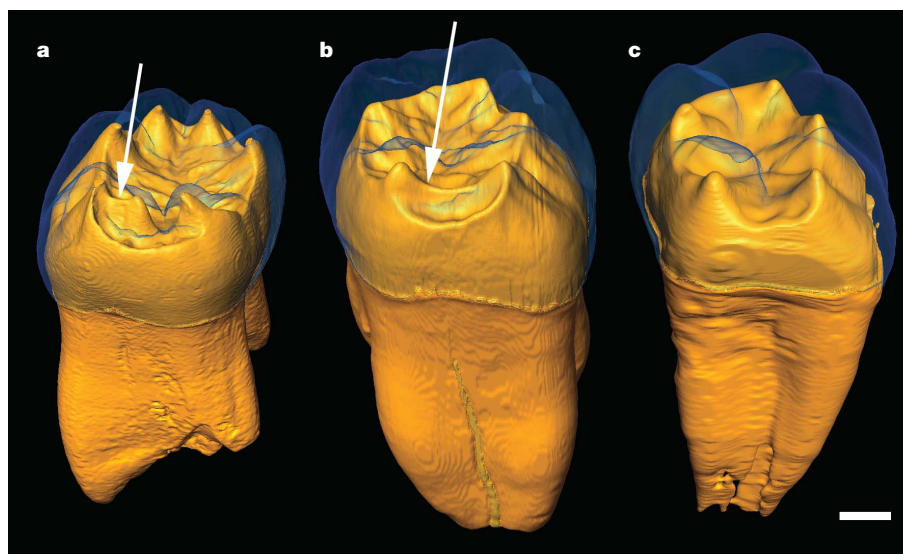


**Figure 1 | SR- $\mu$ CT-based three-dimensional virtual reconstruction of deciduous and permanent Neanderthal molars from La Chaise.** The transparent enamel caps are compared with a modern human permanent molar (slightly oblique mesiobuccal views). **a**, Neanderthal lower right deciduous second molar (LRm2). **b**, Neanderthal lower left permanent first molar (LLM1). **c**, Modern human lower M1. In each of the molars from La

Chaise, the metaconid, or mid-trigonid, crest (arrow), typical of Neanderthals but rare in modern humans, runs in both dentine and enamel between the two anterior cusps (metaconid and protoconid); in the deciduous molar the crest is divided<sup>11</sup>. The feature is absent from the modern human specimen. Scale bar, 2 mm.

<sup>1</sup>Laboratoire de Géobiologie, Biochronologie et Paléontologie Humaine, UMR 6046 CNRS, Université de Poitiers, 86022 Poitiers, France. <sup>2</sup>Sezione di Antropologia, Museo Nazionale Preistorico Etnografico 'L. Pigorini', 00144 Rome, Italy. <sup>3</sup>Université de Perpignan, 66000 Perpignan, France. <sup>4</sup>Etudes Recherches Matériaux, 86022 Poitiers, France. <sup>5</sup>Musée d'Angoulême, 16000 Angoulême, France. <sup>6</sup>UMR 5199 CNRS, Université Bordeaux 1, 33405 Bordeaux, France. <sup>7</sup>Department of Anatomy and Developmental Biology, University College London, London WC1E 6BT, UK.

more complex EDJ topography relative to the enamel surface area in both deciduous and permanent Neanderthal teeth (Supplementary Table 1). The percentage ratio between EDJ area and enamel surface area suggests that both modern human and Neanderthal deciduous molars have proportionately greater EDJ surface areas than permanent molars. However, both deciduous and permanent Neanderthal molars show a more complex EDJ than is typical of modern humans<sup>12</sup>, with about 10% greater surface area. Larger sample sizes will be required to confirm this and focus further on how this might relate to function<sup>13,14</sup>. We then used thin ground sections of the same molar teeth and polarized light microscopy to compare the subsequent timing of enamel formation, crown completion and root formation with times known for modern humans of diverse geographical origins<sup>15,16</sup>.

There has been speculation, but no data, for the timing of molar tooth formation and gingival emergence in Neanderthals<sup>17–20</sup>. We made direct counts and measurements of daily enamel cross-striations to retrieve information about the timing and rate of enamel formation. Birth is marked in deciduous teeth and first permanent molars by an accentuated neonatal line. The position of this line depends upon the time of initial mineralization *in utero* as well as on the time of birth. Enamel secretion rates through the first-formed cuspal enamel of the Neanderthal deciduous molar (Fig. 2) show a slight gradient from the EDJ to the enamel surface (increasing as modern humans do from between 2 or 3  $\mu\text{m}$  per day to about 4  $\mu\text{m}$  per day) but with the typical postnatal hypoplasia and decrease in daily rates of formation during the immediate period after birth. The position of the neonatal line and duration of this reaction to the changing physiology at birth is similar to that in modern humans<sup>21</sup>.

Enamel secretion rates through the first-formed cuspal regions of the Neanderthal permanent molar teeth (Fig. 3) show a steeper gradient than in deciduous teeth, exactly as in modern humans<sup>22</sup> but with slightly higher rates at the EDJ (increasing from about 3  $\mu\text{m}$  per day rather than about 2.5 to about 5  $\mu\text{m}$  per day). The total crown formation times in both deciduous and permanent molars were nearly identical with those reported for large samples of modern humans<sup>15,16</sup>. Protoconid initiation in the M1 occurred about 15 days before birth (neonatal line) and metaconid initiation about 18 days

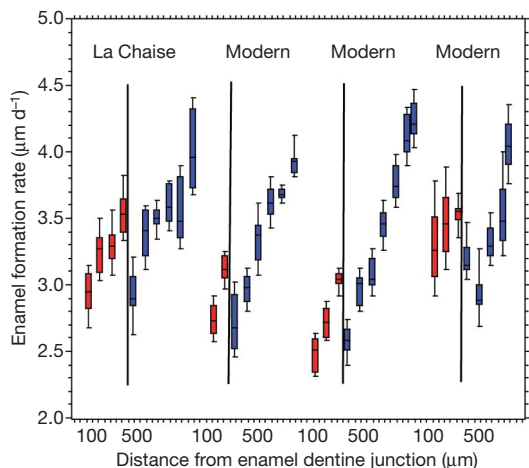


**Figure 2 | Graphs of deciduous second molar enamel formation rates for the Neanderthal and three typical modern human deciduous molars.** Each box plot is for a minimum of ten groups of five cross-striations averaged at 100- $\mu\text{m}$  zones of enamel as measured from the EDJ (the horizontal lines in each box show 25th, 50th and 75th centiles. The whiskers indicate 10th and 90th centiles). The vertical black line indicates the position of the neonatal line with respect to the EDJ and the measurements of daily secretion rates (red, prenatal; blue, postnatal). The positions of the neonatal line and the recovery phase after birth are similar. In the Neanderthal, the neonatal line occurred about 60 days after initiation in the metaconid and about 100 days in the protoconid. The total crown formation time was about 315 days.

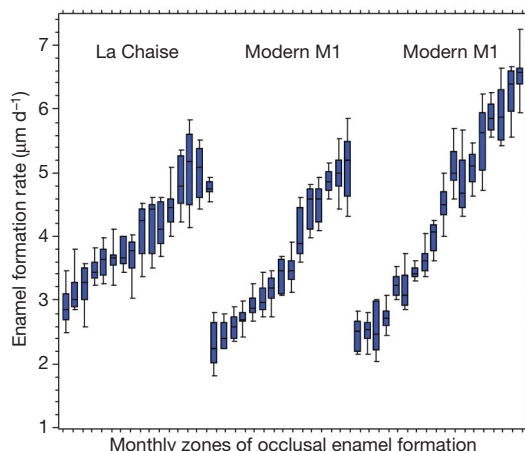


**Figure 3 | Graphs of daily occlusal enamel formation rates in the permanent Neanderthal M1 and in modern human molars.** Daily rates are averaged as a box plot (with elements defined as in Fig. 2) for successive months of occlusal enamel formation in each molar and are essentially similar. There is a steep gradient of increase in enamel formation rates in all cases. Mean values of measurements in the first monthly zone ( $n = 57$  from four modern human molars) were  $2.4 \pm 0.3 \mu\text{m}$  per day (mean  $\pm$  s.d.). In Neanderthals, rates during the first month were slightly higher and closer to 3  $\mu\text{m}$  per day. Measurements in the M1 from La Chaise ( $n = 13$ ) were  $2.9 \pm 0.4 \mu\text{m}$  per day and in Tabun C1 (ref. 18) ( $n = 10$ ) they were  $3.2 \pm 0.4 \mu\text{m}$  per day. Maximum rates at the surface enamel increase to about 5 or 6  $\mu\text{m}$  per day in both Neanderthals and modern humans.

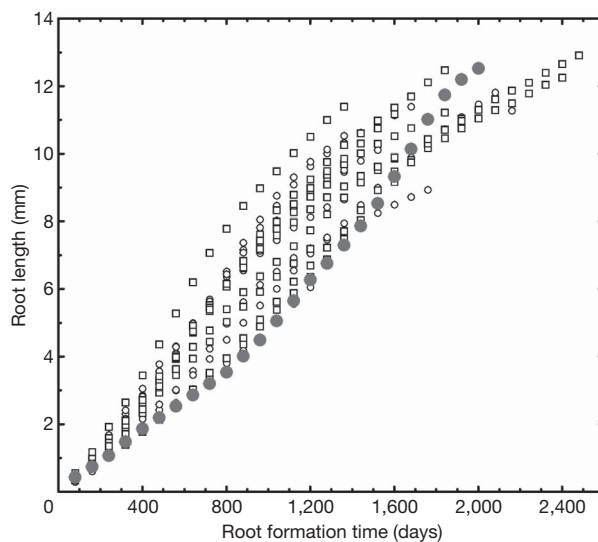


**Figure 4 | Growth curves for roots of M1 for 20 modern humans (by sex) and the Neanderthal M1.** No differences exist in the distribution of faster or slower growth curves between sexes in modern humans (open circles, females; open squares, males). The Neanderthal root (filled circles) has a slower than average trajectory for the first two-thirds of root growth but then rises quickly towards the end of root growth. The combined time of protoconid formation in La Chaise M1 (1,041 days) and root formation (2,119 days) totals 3,160 days or about 105 months (about 8.7 years). The average extension rate was 6.3  $\mu\text{m}$  per day over a root length of 13.3 mm. The root formation stage in La Chaise M1 was just short of complete closure at the time of death. Estimates of the mean age of attainment of M1 apex formation in modern humans with the ‘root canal terminally divergent’ (that is, just short of completion) were 100 months, or 8.3 years, in boys (s.d. 7.7 months) and 94.1 months, or 7.8 years, in girls (s.d. 8.1 months) with a mean extension rate for the whole M1 root of 6.8  $\mu\text{m}$  per day (ref. 23). In ref. 23, M1 root formation was, on average, complete at 106.6 months (8.9 years) in boys and 102.5 months (8.54 years) in girls.

after birth. The protoconid took about 1,041 days to form to the cervix and the metaconid about 865 days to the cervix, both only slightly below 1 s.d. of the mean for modern humans of African origin ( $1,117 \pm 55$  and  $936 \pm 55$  days). Protoconid lateral enamel formation took about 645 days and expressed about 90 surface perikymata with a periodicity of 7 days.

The timing of root completion in the Neanderthal M1 from La Chaise was reconstructed from incremental markings in the dentine<sup>7</sup>. M1 root completion occurs at about 9 years in modern humans<sup>23</sup> but has not previously been known for Neanderthals. We report here that closure of the root apex was occurring as in modern humans at about 8.7 years of age in this Neanderthal. However, Neanderthal molars are typically taurodont with a long root trunk and with late bifurcation or trifurcation of the roots. Rates of M1 root elongation (root extension<sup>24</sup>) in modern humans and in this Neanderthal differ (Fig. 4), with slow early root extension rates and a very late peak or spurt shortly after root bifurcation in the Neanderthal (Fig. 5).

Counts and packing patterns of perikymata on anterior tooth surfaces show that the large incisors and canines of Neanderthals formed more quickly than in some modern humans<sup>4,5</sup>. Periodicities of perikymata determined in this study and from Tabun C1 (ref. 18) (7 and 8 days, respectively) bolster these conclusions. However, gingival emergence of the first permanent molar is a more reliable measure of relative dental development than are anterior tooth crown formation times and is also tightly correlated with brain size in anthropoid primates<sup>1,2</sup>. Our data now allow us to predict M1 emergence time in Neanderthals with more certainty. If about 8 mm of root were formed at an average of about 5.7  $\mu\text{m}$  per day at gingival emergence, then this would have occurred at about 6.7 years of age, well within the human range ( $6.2 \pm 0.8$  years (mean  $\pm$  s.d.))<sup>23</sup>. This, together with the modern human-like position of the neonatal line, suggests both similar timing of tooth initiation relative to birth in Neanderthals and modern humans, and a predictable extended period between birth and M1 emergence, by which time about 90% of brain volume would have been attained<sup>1,25</sup>.

One hundred and fifty years after the discovery of the Neanderthal type specimen, the prospects for further work on the complex relationships between jaw size and jaw growth<sup>26</sup>, early permanent molar initiation<sup>27,28</sup> and those factors that underlie rates of tooth eruption

that are faster than usual<sup>29</sup> are good. Moreover, improved imaging techniques<sup>30</sup> combined with further histological analyses of deciduous and permanent tooth enamel are likely to reveal evidence for any changing patterns of perinatal stress as Neanderthals approached extinction and so provide critical evidence about the shift in balance between adult mortality rates, fertility rates and infant survival among more recent Neanderthals than those at La Chaise.

## METHODS

**Micro-computed tomography analysis.** Virtual three-dimensional reconstructions and measurements (Supplementary Information) are based on a high-resolution SR- $\mu\text{CT}$  record performed at the beamline ID17 set at the European Synchrotron Radiation Facility, Grenoble (<http://www.esrf.fr/UsersAndScience/Experiments/Imaging/ID17/>; experiments SC-1587 and SC-1749). The system is characterized by a continuous energy spectrum, a high photon flux, an intense monochromatic X-ray beam, nearly parallel projections and a small angular source size. Samples are located about 140 m from the source point. Monoenergetic X-ray beams enable absolute linear attenuation coefficients to be measured and avoid the risk of beam-hardening artefacts in the reconstruction of images from dense specimens such as highly mineralized fossils<sup>30</sup>. Scans of the two Neanderthal teeth from La Chaise were performed at energies of 51 keV (deciduous) and 70 keV (permanent). Projections (of 22.6 and 25.6 ms for the deciduous tooth and the permanent tooth, respectively) were taken every  $0.12^\circ$  and were collected by a  $2,048 \times 2,048$  fibre-optical taper charge-coupled device Frelon camera. Final sections were reconstructed from sinograms and saved in a 32-bit floating-point raw format at a resolution (voxel size) of  $45.5 \times 45.5 \times 45.7 \mu\text{m}^3$ . The final eight-bit volumes ( $239 \times 262 \times 351$  pixels for the deciduous molar and  $493 \times 357 \times 237$  pixels for the permanent molar) were analysed by means of AMIRA v. 4.0 (Mercury Computer Systems, Inc.). Segmentation of the volume was done semi-automatically with manual corrections. The original SR- $\mu\text{CT}$  record is available at the NESPOS website (<https://nespos.pitcom.net/display/openspace/Home>).

**Histological analysis.** Longitudinal ground sections of molars were prepared in the buccolingual plane. The plane of section passed through the mesial cusps, the last-formed enamel at the mesiobuccal cervix and through the long axis of the root. Often, the apical portion of the root turned distally with respect to this plane of section and was therefore cut obliquely thereafter. Only sections with at least 10 mm of root true to the plane of section were included in this study. An initial 200–300- $\mu\text{m}$  slice was made with a circular diamond saw. Each slice was lapped and polished to a roughly 80- $\mu\text{m}$ -thick section then cleaned and mounted for routine polarized light microscopy. Additional details about calculating root extension rates are provided in Supplementary Information.

Received 20 July; accepted 3 October 2006.

Published online 22 November 2006.

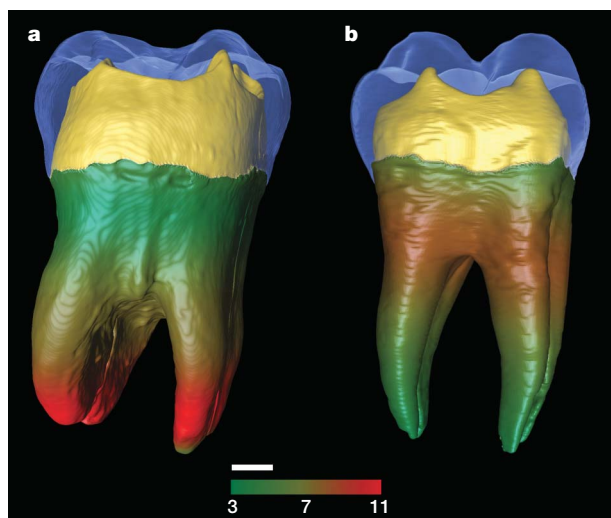


**Figure 5** | SR- $\mu\text{CT}$ -based three-dimensional visualization of the differences in root extension rate. **a**, The Neanderthal M1 from La Chaise. **b**, An average modern human lower M1. Both are in lingual view. The pseudo-colour scale, ranging from dark green (3  $\mu\text{m}$  per day) to red (11  $\mu\text{m}$  per day), is used to render the topographic variation of the root extension rate from the cervix (yellow–green boundary) towards the radicular apex of the tooth. Extension rate data are from Supplementary Fig. 5. Scale bar, 2 mm.

- Smith, B. H. Dental development and the evolution of life history in Hominidae. *Am. J. Phys. Anthropol.* **86**, 157–174 (1991).
- Smith, B. H. & Tompkins, R. L. Towards a life history of the Hominidae. *Annu. Rev. Anthropol.* **24**, 257–279 (1995).
- Avishai, G. et al. New approach to quantifying developmental variation in the dentition using serial microtomographic imaging. *Microsc. Res. Tech.* **65**, 263–269 (2004).
- Ramirez-Rozzi, F. V. & Bermudez de Castro, J. M. Surprisingly rapid growth in Neanderthals. *Nature* **428**, 936–939 (2004).
- Guatelli-Steinberg, D., Reid, D. J. & Bishop, T. A. Anterior tooth growth periods in Neanderthals were comparable to those in modern humans. *Proc. Natl Acad. Sci. USA* **102**, 14197–14202 (2005).
- Debénath, A. *Néanderthaliens et Cro-Magnons. Les Temps Glaciaires dans le Bassin de la Charente* (Le Croît Vif, Paris, 2006).
- Dean, M. C. Comparative observations on the spacing of short-period (von Ebner's) lines in dentine. *Archs Oral Biol.* **43**, 1009–1021 (1998).
- Dean, M. C. Tooth microstructure tracks the pace of human life-history evolution. *Proc. R. Soc. B* **273**, 2799–2808 (2006).
- Jernvall, J. & Thesleff, I. Reiterative signalling and patterning in mammalian tooth morphogenesis. *Mech. Dev.* **92**, 19–29 (2000).
- Thesleff, I., Keranen, S. & Jernvall, J. Enamel knots as signalling centers linking tooth morphogenesis and odontoblast differentiation. *Adv. Dent. Res.* **15**, 14–18 (2001).
- Bailey, S. E. A closer look at Neanderthal postcanine dental morphology: The mandibular dentition. *Anat. Rec. (New Anat.)* **269**, 148–156 (2002).
- Kono, R. T. Molar enamel thickness and distribution patterns in extant great apes and humans: New insights based on a 3-dimensional whole crown perspective. *Anthropol. Sci.* **112**, 121–146 (2004).
- Olejniczak, A., Martin, L. B. & Ulhaas, L. Quantification of dentine shape in anthropoid primates. *Ann. Anat.* **186**, 479–485 (2004).

14. Suwa, G. & Kono, R. T. A micro-CT based study of linear enamel thickness in the mesial cusp section of human molars: Reevaluation of methodology and assessment of within-tooth, serial, and individual variation. *Anthropol. Sci.* **113**, 273–289 (2005).
15. Liversidge, H. M. & Molleson, T. Variation in crown and root formation and eruption of human deciduous teeth. *Am. J. Phys. Anthropol.* **123**, 172–180 (2004).
16. Reid, D. J. & Dean, M. C. Variation in modern human enamel formation times. *J. Hum. Evol.* **50**, 329–346 (2006).
17. Dean, M. C., Stringer, C. B. & Bromage, T. G. Age at death of the Neanderthal child from Devils Tower, Gibraltar and the implications for studies of general growth and development in Neanderthals. *Am. J. Phys. Anthropol.* **70**, 301–309 (1986).
18. Stringer, C. B., Dean, M. C. & Martin, R. D. in *Primate Life History and Evolution: Monographs in Primatology* Vol. 14 (ed. De Rousseau, C. J.) 115–152 (Wiley-Liss, New York, 1990).
19. Trinkaus, E. & Tompkins, R. L. in *Primate Life History and Evolution: Monographs in Primatology* Vol. 14 (ed. De Rousseau, C. J.) 153–180 (Wiley-Liss, New York, 1990).
20. Tillier, A.-M., Mann, A. E., Monge, J. & Lampl, M. L'ontogenèse, la croissance de l'émail dentaire et l'origine de l'homme moderne: l'exemple des Néandertaliens. *Anthropol. Préhist.* **106**, 97–104 (1995).
21. Rossi, P. F., Bondioli, L., Geusa, G. & Macchiarelli, R. in *Digital Archives of Human Paleobiology* (eds Bondioli, L. & Macchiarelli, R.) (E-LISA, Milano, 1999) [CD-ROM].
22. Dean, M. C. *et al.* Growth processes in teeth distinguish modern humans from *Homo erectus* and earlier hominins. *Nature* **414**, 628–631 (2001).
23. Gleiser, I. & Hunt, E. E. The permanent mandibular molar: Its calcification, eruption and decay. *Am. J. Phys. Anthropol.* **13**, 253–283 (1955).
24. Shellis, R. P. Variations in growth of the enamel crown in human teeth and a possible relationship between growth and enamel structure. *Archs Oral Biol.* **29**, 697–705 (1984).
25. Ashton, E. H. & Spence, T. F. Age changes in the cranial capacity and foramen magnum of hominoids. *Proc. Zool. Soc. Lond.* **130**, 169–180 (1958).
26. Kondo, O. *et al.* in *Current Trends in Dental Morphology Research* (ed. E. Żądzińska) 243–255 (Univ. Lodz Press, 2005).
27. Boughner, J. C. & Dean, M. C. Does space in the jaw influence the timing of molar crown initiation? A model using baboons and great apes. *J. Hum. Evol.* **46**, 253–275 (2004).
28. Tompkins, R. L. Relative dental development of Upper Pleistocene hominids compared to human population variability. *Am. J. Phys. Anthropol.* **99**, 103–118 (1996).
29. Wolpoff, M. H. The Krapina dental remains. *Am. J. Phys. Anthropol.* **50**, 67–114 (1979).
30. Mazurier, A., Volpato, V. & Macchiarelli, R. Improved noninvasive microstructural analysis of fossil tissues by means of SR-microtomography. *Appl. Phys. A* **83**, 229–233 (2006).

**Supplementary Information** is linked to the online version of the paper at [www.nature.com/nature](http://www.nature.com/nature).

**Acknowledgements** We thank A. Bravin, C. Nemoz and P. Tafforeau for collaboration at the ESRF beamline ID17; the Centre de Microtomographie (CdMT) at the University of Poitiers; the Department of Physics at the University of Bologna; and P. Bayle, A. Bergeret, P. Sardini, V. Volpato and P. Walton for technical assistance. The research was supported by the French CNRS, the EU TNT Project (to R.M.), the Région Poitou-Charentes (to A.M.), and The Leverhulme Trust and The Royal Society (to C.D.).

**Author Information** Reprints and permissions information is available at [www.nature.com/reprints](http://www.nature.com/reprints). The authors declare no competing financial interests. Correspondence and requests for materials should be addressed to C.D. ([ucgacrd@ucl.ac.uk](mailto:ucgacrd@ucl.ac.uk)).